PHYSICAL REVIEW B VOLUME 11, NUMBER 8 15 APRIL 1975

Shell-model calculation of some point-defect properties in α–Al_2O_3†

G. J. Dienes and D. O. Welch
Brookhaven National Laboratory, Upton, New York 11973

C. R. Fischer, R. D. Hatcher, O. Lazareth,* and M. Samberg
Queens College, City University of New York, Flushing, New York 11367
(Received 25 November 1974)

A polarizable point-ion shell model has been developed for α–Al_2O_3. The material is treated as perfectly ionic, the repulsive interactions were calculated from free-ion wave functions, and the single empirical parameter of the model was obtained from an analysis of dielectric data. The model yields a good account of the cohesive properties of the perfect crystal. Calculations of the formation energy of vacancies and interstitials predict that Schottky defects are energetically more favorable than Frenkel pairs. Preliminary calculations of defect motion energies suggest that O^{2-} vacancies are the most mobile defect. Existing data on diffusion and radiation-damage annealing are reviewed in light of the calculations.

I. INTRODUCTION

There is considerable interest in the refractory oxides for a variety of high-temperature and nuclear applications. The defect structure of these materials is of great importance for atomic transport and for response to high-energy radiation. Aluminum oxide, Al_2O_3, may be considered a prototype suitable for theoretical study. Some experimental information is available on Al_2O_3 from diffusion and radiation-damage studies, but the intrinsic and mobile defects have not been identified. It is important, therefore, to estimate theoretically the formation and migration energies of aluminum and oxygen vacancies and interstitials.

The interpretation of the available experimental information is by no means clear cut. The data are rather meager since high-temperature experimentation is difficult. Further, very little is known about impurities in Al_2O_3, and these can play a very important role in defect formation and motion. The single-crystal experiments of Oishi and Kingery[1] for oxygen diffusion are most easily interpreted. The over-all activation energy for diffusion of oxygen E_D at high temperature was measured as 6.6 eV while at low temperature E_D was 2.5 eV. If one assumes that oxygen migration alone was measured in the low-temperature extrinsic region, then one can assign 2.5 eV to the oxygen migration energy E_M. If one now assumes that stoichiometric oxygen and aluminum vacancies are the dominant defects (three O^{2-} vacancies and two Al^{3+} vacancies for electrical neutrality), then the Schottky formation energy E_F is given by $E_D = \frac{1}{5}E_F + E_M$, yielding $E_F = 20.5$ eV or 4.1 eV per defect. Oxygen diffusion in a polycrystalline sample was characterized by a considerably lower E_D of 4.8 eV, about the same E_D value as found for aluminum diffusion in a polycrystalline sample.[2] With no single-crystal data reported for aluminum diffusion, it is difficult to estimate the migration energy for aluminum.

It should be mentioned that Fryer,[3] on the basis of sintering experiments with doped and undoped samples, suggested quite a different assignment of energies, since he concluded that the high-temperature oxygen-diffusion experiment above was impurity controlled. Without further experiments a clear conclusion is impossible.

Most of the experiments[4] on the annealing of radiation damage indicate activation energies near 2.2 eV, which presumably characterizes the fastest moving defect. It should be noted, however, that two activation energies have also been suggested, 1.2 and 3.4 eV, for describing annealing in the (400–1400) °C temperature range.[5]

It is clear that not only is further experimentation necessary, but in addition theoretical studies are required to clarify the nature of the point defects responsible for atomic transport and the annealing of radiation damage. Calculations are presented in this paper based on a polarizable point-ion shell model for α-Al_2O_3 with the major aim of determining defect formation energies and hence the intrinsic defects expected on the basis of energetics. The symmetry and surroundings of simple defects are outlined in Sec. II. The determination of a suitable shell model for Al_2O_3 is discussed in Sec. III, and the properties of the perfect crystal based on this model are presented in Sec. IV. The calculations and results for the formation energies of vacancies (Schottky defects) and interstitials (Frenkel pairs) are given in Sec. V, together with some estimates of activation energies for some likely migration paths. The results are summarized and discussed in Sec. VI.

TABLE I. Cartesian coordinates of the ions in a unit cell of $\alpha-Al_2O_3$ in units of $a = 5.124$ Å. The origin of the coordinate system is located at the center of mass of the unit cell (the vertex in Fig. 2).

Ion	Type	X	Y	Z
1	Al	0	0	0.3750
2	O	−0.2457	−0.1418	0.6334
3	O	0.2457	−0.1418	0.6334
4	O	0	0.2837	0.6334
5	Al	0	0	0.8918
6	Al	0	0	−0.3750
7	O	0.2457	0.1418	−0.6334
8	O	−0.2457	0.1418	−0.6334
9	O	0	−0.2837	−0.6334
10	Al	0	0	−0.8918

II. STRUCTURE OF α-Al_2O_3 AND THE SYMMETRY OF VACANCIES AND INTERSTITIALS

The structure of α-Al_2O_3, space group D_{3d}^6, may be described as a slightly distorted hexagonal-close-packed arrangement of oxygen ions (O^{2-}) with the aluminum ions (Al^{3+}) occupying two-thirds of the interstices.[6] A sketch, neglecting the distortion from the "ideal" hexagonal-close-packed structure, is shown in Fig. 1, with the Al^{3+} ions shown on lines perpendicular to the close-packed planes of oxygen ions. The X's indicate the positions where these lines intersect the planes. The primitive unit cell is a rhombohedron of side 5.124 Å and vertex angle 55° 17′, as shown in Fig. 2. The basis is a group of two molecules centered around the vertex. The Cartesian coordinates of 10 typical ions are listed in Table I.

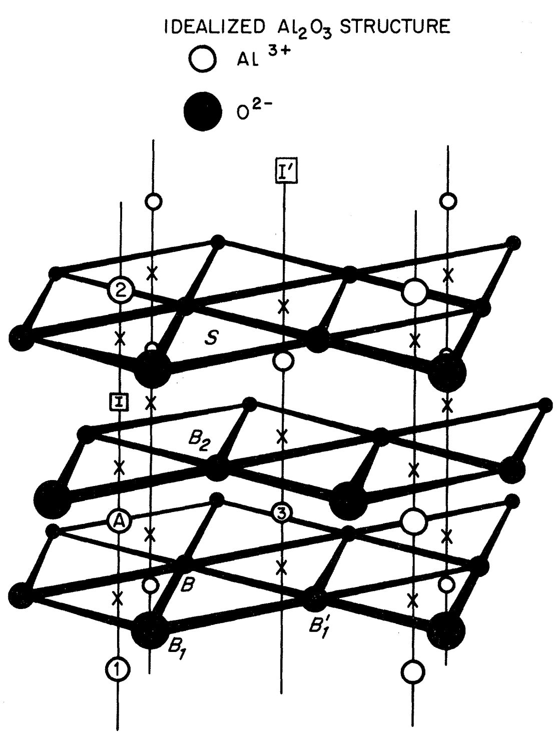

FIG. 1. Idealized α-Al_2O_3 structure. A and B indicate the sites of aluminum and oxygen vacancies, and I is the octahedral interstitial site. Other symbols are defined in Section V B.

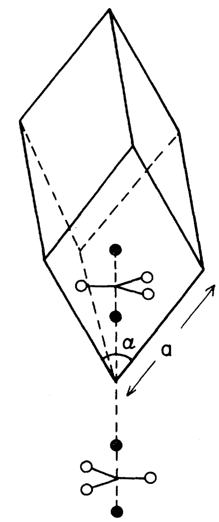

FIG. 2. Primitive unit cell and basis for α-Al_2O_3.

An Al^{3+} vacancy is located at position A in Fig. 1. Its nearest neighbors are two sets of three O^{2-} ions, at distances of 1.86 and 1.97 Å, as shown in Fig. 3. An O^{2-} vacancy is located at position B in Fig. 1, surrounded by two Al^{3+} ions at 1.86 Å and two at 1.97 Å, arranged roughly in a tetrahedron around the O^{2-} vacancy, as sketched in Fig. 4. The most likely site for an interstitial ion is at position I the octahedral interstitial site, in Fig. 1. As sketched in Fig. 5, the octahedral interstitial site has two Al^{3+} neighbors at 1.92 Å and six O^{2-} neighbors at 1.98 Å.

III. SHELL MODEL FOR Al_2O_3

For the purposes of this calculation, it has been assumed that the properties of point defects in Al_2O_3 can be calculated by treating the material as perfectly ionic and by describing the cohesive properties by means of a polarizable point-ion shell model. In this model the energy of the crystal in any structural configuration is the sum of Coulombic (monopole and dipole), closed-shell repulsive, and Van der Waals's interactions. The legitimacy of such a model for Al_2O_3 depends, of course, on the degree of agreement of its predictions with experi-

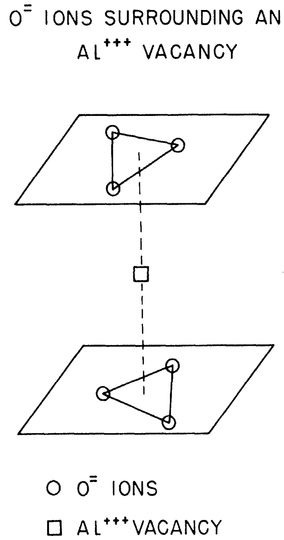

FIG. 3. Nearest neighbors to Al^{3+} vacancy.

mental results. First a description of the details of the model will be given in this section, followed by a comparison, in Sec. IV, between the predictions of the model and experimental data for the perfect crystal.

A. Madelung energy

The monopole-monopole Coulombic interactions contribute the Madelung energy

$$E_m = \frac{1}{2} \sum_{i,j}^{N}{}' \frac{q_i q_j}{r_{ij}} \tag{1}$$

to the total energy, where q_i, q_j are the ionic charges and r_{ij} is the separation of ions i and j. N is the number of ions in the crystal. Equation (1) can be rewritten for an infinite crystal as

$$E_m = \frac{1}{2}\sum_i q_i\phi_i = \frac{1}{2}\sum_i q_i(\phi_i^0 + \Delta\phi_i), \tag{2}$$

where ϕ_i is the site potential for ion i, ϕ_i^0 is the site potential for an infinite crystal with all ions present either in perfect-crystal lattice or interstitial positions, and $\Delta\phi_i$ is the change in the Madelung potential when an ion moves from a perfect-crystal position (i.e., when the lattice relaxes around a defect). In this calculation, the infinite-crystal rigid-lattice site potentials ϕ_i^0 were calculated by the method of Bartram,[7] and the changes in potential due to lattice relaxation $\Delta\phi_i$ were calculated by direct summation over the ions of a finite crystallite containing 1855 ions. While substantial deviations from results for an infinite crystal can occur with finite sums for the site potential itself,[8] much smaller errors will occur in $\Delta\phi$ when it is calculated by finite summation. For example, the $q\Delta\phi$ which results when an Al^{3+} ion is displaced from its perfect crystal position, in an otherwise perfect infinite crystal, to the octahedral interstitial site, from A to I in Fig. 1, is 33.4 eV, while the same displacement in the center of the 1855 ion crystallite results in a value of 33.5 eV. The actual relaxations around the defects considered here are much smaller than the displacement in the example above, $\lesssim 0.25$ Å compared with 1.92 Å above, thus the error per relaxed ion is probably less than about 0.01 eV. For 30 relaxed ions, typical of these calculations, the total error in the formation energy is less than about 0.3 eV. (This is probably an overestimate since the discrepancy in $q\Delta\phi$ for displacing an O^{2-} ion from B_1 to I in Fig. 1 is zero.) Several site energies $q\Delta\phi^0$ for an infinite perfect crystal are listed in Table II. The Madelung contribution to the cohesive energy, per Al_2O_3 "molecule," is given by $E_m^{\text{coh}} = -3e(\phi_{\text{Al}}^0 + \phi_{\text{ox}}^0)$ and amounts to 189.1 eV.

B. Closed-shell repulsive energy

The repulsive interactions between the closed electronic shells of ions are generally approximated by some variation of the Born-Mayer potential, the parameters of which are determined from perfect crystal properties such as cohesive energy, equilibrium crystal volume, compressibility, etc.[9] No such analysis has yet been performed for Al_2O_3, and alternatively these interactions were calculated from the wave functions of the free ions using a modification[10] of the method, reputedly invented by Lenz and Jensen[11] and periodically rediscovered.[12,13] Recently, this approach has been shown[13] to give good results for alkali-halide crystals, comparable with the empirical Born-Mayer approach, and approximates the interaction by the sum of potential, kinetic, and exchange energies of an interacting ion

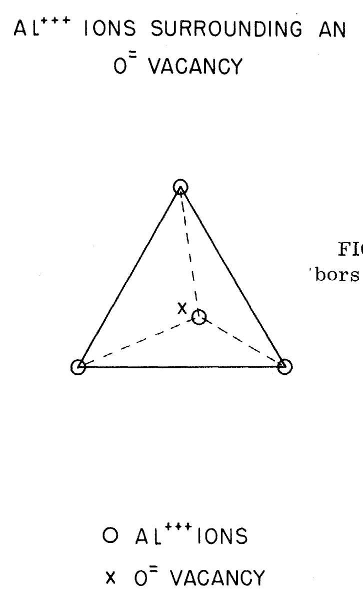

FIG. 4. Nearest neighbors to O^{2-} vacancy.

TABLE II. Contributions to the potential energy of ions in various sites of a perfect crystal of α-Al_2O_3. (All energies in eV.)

Ion and site	Madelung energy	Repulsive energy	Van der Waals's energy	Total potential energy
Al^{3+}, lattice site	−109.8	+19.5	−0.1	−90.4
O^{2-}, lattice site	−52.8	+13.0	−1.3	−41.1
Al^{3+}, octahedral interstitial	−8.9	+16.0	−0.1	+7.0
O^{2-}, octahedral interstitial	+5.9	+9.4	−3.6	+11.7

pair calculated from the electron density, obtained from free-ion wave functions. The density dependence of the kinetic and exchange energies is taken to be that of a free electron gas.

The wave functions used for the Al^{3+} ion were those of Clementi,[14] while those of O^{2-} were calculated by Watson[15] for an ion in a spherical well of charge +1. The resulting interaction energy for O^{2-} ion pairs and for Al^{3+}-O^{2-} ion pairs is shown in Fig. 6, together with an empirical O^{2-}-O^{2-} interaction obtained by Huggins and Sakamoto[16] (HS) from an analysis of cohesive data for the alkaline-earth oxides, shown for comparison. The total repulsive energy of the crystal is then given by

$$E_{\text{rep}} = \frac{1}{2} \sum_{i,j}{}' \phi^{(r_{ij})}_{\text{repulsive}} = \frac{1}{2} \sum_{i,j}{}' A_{ij} e^{-B_{ij} r_{ij}} , \qquad (3)$$

where the Born-Mayer parameters A and B appropriate to particular ion pairs and designated ranges of separation r_{ij} were obtained by fitting the numerical results of the Wedepohl procedure, shown in Fig. 6. These parameters are collected in Table III. Evidence for the accuracy of these interactions in accounting for perfect crystal cohesive properties will be discussed in Sec. IV. The contribution of the repulsive interactions to the potential energy of ions in various sites in a perfect crystal is summarized in Table II.

C. Polarization energy

Possibly the most critical component in the calculation of the energy of formation of lattice defects, particularly vacancies, in ionic crystals is the energy of polarization resulting from defect-produced electric fields. For example, in this calculation, about 40% of the energy to remove an Al^{3+} ion from a rigid, unpolarized lattice is recovered when the ions relax their position and their electron clouds polarize. About 75% of this relaxation energy is the energy of polarization. Therefore, the accuracy of point-defect calculations for ionic crystals strongly depends upon the treatment of polarization. There are two aspects of this problem: a suitable microscopic model for the response of a particular ion to a local electric field and the determination of the local field itself, i.e., the treatment of the dipole-dipole interactions. In this calculation, a simple shell model was used to describe local polarizability, and the local field problem was solved by the use of a combination of the matrix method of Dellin *et al.*[17] and the Mott-Littleton approximation for effective polarizabilities.[18]

The desirability of the use of some type of shell model to describe the microscopic dielectric response of crystals containing defects has been discussed by Norgett and Lidiard[19]; in the case of Al_2O_3 this becomes a necessity. The use of constant polarizabilities, e.g., those of Tessman, Kahn, and Shockley,[20] results in an instability of the polarizable point-ion model of Al_2O_3, even for the perfect crystal. In this case, when an Al^{3+} ion

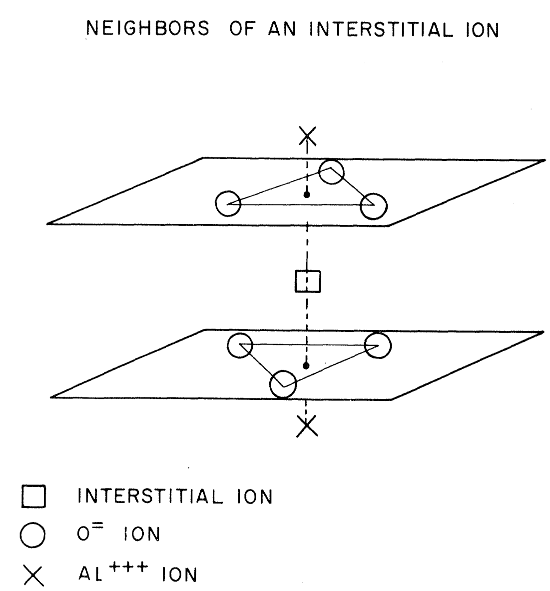

FIG. 5. Nearest neighbors to the octahedral interstitial site.

is displaced toward a neighboring O^{2-} ion, the dipole-dipole interaction force is sufficient to overcome the repulsive forces and a polarization "catastrophe" results. This "catastrophe" does not occur if the coupling of the polarizability of an ion and its surroundings is taken into account, as has been done in lattice dynamical calculations by the use of shell models. Recent calculations[21–23] have shown that simple shell models give a good description of various properties of diatomic molecules, where the electric fields are even larger than in defect crystals, for alkali halides and alkaline earth oxides. Therefore a simple shell model has been employed in this calculation.

Dick and Overhauser[24] introduced the simple shell model by proposing that the outer electrons of an ion are predominantly responsible for both the polarizability and the repulsion due to closed-shell overlap. Thus they described each ion as a rigid shell of charge, coupled with a spring to its core, and coupled by springs to the shells of other ions, thereby accounting, in the harmonic approximation, for the overlap repulsion. The charge of the rigid shell is then expected to be of the order of the number of electrons in the outer closed electronic shell.

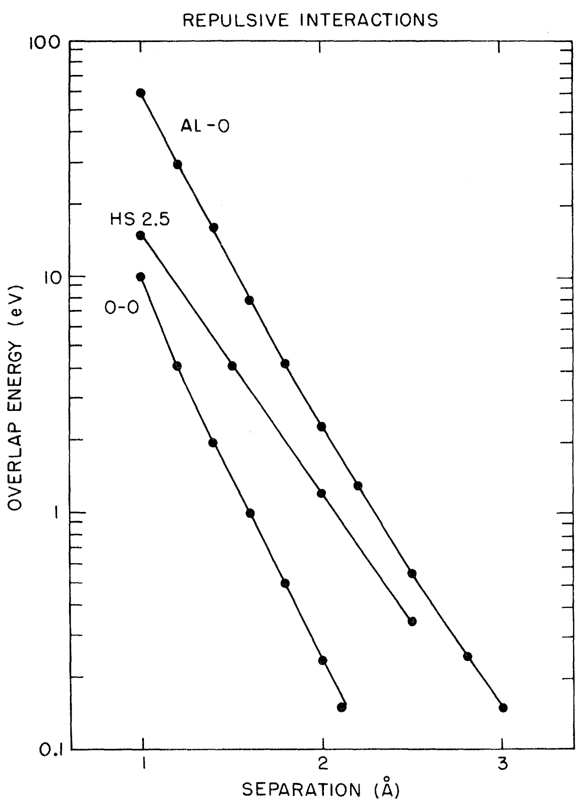

FIG. 6. Repulsive interactions calculated by the modified Wedepohl method.

TABLE III. Born-Mayer constants from a segmented fit to the repulsive interactions for ions in Al_2O_3.

Ion pair	A(eV)	B(Å^{-1})	Range of separation (Å)
Al^{3+}-Al^{3+}	1.268×10^4	7.550	$r<1.3$
	7.775×10^4	10.70	$r\geq1.3$
Al^{3+}-O^{2-}	3.000×10^3	3.917	$r<1.0$
	1.818×10^3	3.416	$1.0\leq r<1.4$
	1.234×10^3	3.139	$1.4\leq r<1.9$
	7.676×10^2	2.889	$1.9\leq r<2.4$
	4.061×10^2	2.630	$2.4\leq r$
O^{2-}-O^{2-}	4.596×10^3	6.498	$r<0.7$
	1.713×10^3	5.089	$0.7\leq r<1.0$
	6.451×10^2	4.170	$1.0\leq r<1.3$
	3.082×10^2	3.580	$1.3\leq r<1.7$
	5.657×10^2	3.920	$1.7\leq r<2.06$
	1.597×10^5	6.609	$2.06\leq r$

An analagous approach,[21] which reduces to the Dick-Overhauser model in a harmonic approximation and to the deformation dipole model of Hardy[25] in a linear approximation, is to assume that the effect of an electric field induced distortion of the ionic electron clouds on the overlap repulsion between a pair of ions is to replace the interionic separation r_{ij} in the repulsive interaction potential for undistorted ions by an effective separation r_{ij}^{eff}:

$$\phi^{(r_{ij})}_{\text{repulsive, distorted}}=\phi^{(r_{ij}^{\text{eff}})}_{\text{repulsive, undistorted}} \tag{4}$$

where r_{ij}^{eff} is a function of the multipole moments of the distorted ions. The potential function $\phi_{\text{undistorted}}$ is to be approximated by a Born-Mayer function, or obtained by a Wedepohl-type calculation, for example. The simplest possible form for r_{ij}^{eff} is a linear dependence upon only the dipole moments $\vec{\mu}_i$, $\vec{\mu}_j$:

$$\vec{r}_{ij}^{\text{eff}}=\vec{r}_{ij}+\frac{\vec{\mu}_i}{Q_i}-\frac{\vec{\mu}_j}{Q_j}, \tag{5}$$

where the proportionality constants Q_i^{-1}, Q_j^{-1} are to be determined empirically, and the direction of the vector $\vec{r}_{ij}$ is from i to j. (Including quadrupole moment terms in r^{eff} will lead to a breathing shell model.)

In this scheme, the energy of the polarized crystal excluding Van der Waals's contributions, is

$$E=E_m+\frac{1}{2}\sum_{i,j}{}'\,\phi^{(r_{ij}^{\text{eff}})}_{\text{repulsive}}-\sum\vec{\epsilon}_i^{\,m}\cdot\vec{\mu}_i-\frac{1}{2}\sum_{i,j}{}'\,\frac{3(\vec{\mu}_i\cdot\vec{r}_{ij})(\vec{\mu}_j\cdot\vec{r}_{ij})r_{ij}^2\vec{\mu}_i\cdot\vec{\mu}_j}{r_{ij}^5}+\frac{1}{2}\sum_i\frac{\mu_i^2}{\alpha_i^0}, \tag{6}$$

where $\vec{\epsilon}_i^{\,m}$ is the electric field at i, due to monopoles and applied fields only, and the final term is the self-energy of polarization, with α_i^0 polarizability of the free ion. The last three terms are explicitly the "energy of polarization."

The equilibrium dipole moments are obtained by minimizing the crystal energy with respect to the components of individual dipole moments, e.g., $\partial E/\partial \mu_i^x = 0$, etc. Using the Born-Mayer form for the repulsive energy, Eq. (3), the equilibrium obtained by minimizing with respect to the x component of the ith dipole moment, for a fixed arrangement of ions, followed by expanding the exponentials which include dipole moments to first order in $\vec{\mu}$, yields

$$\mu_i^x\left(\frac{1}{\alpha_i^0}+\sum_{j\neq i}\frac{(e_{ij}^x)^2B_{ij}^2A_{ij}e^{-B_{ij}r_{ij}}}{Q_i^2}\right)+\mu_i^y\left(\sum_{j\neq i}\frac{e_{ij}^x e_{ij}^y B_{ij}^2A_{ij}e^{-B_{ij}r_{ij}}}{Q_i^2}\right)+\mu_i^z\left(\sum_{j\neq i}\frac{e_{ij}^z e_{ij}^x B_{ij}^2A_{ij}e^{-B_{ij}r_{ij}}}{Q_i^2}\right)$$
$$=\epsilon_{i,\,\mathrm{loc}}^x+\sum_{j\neq i}\frac{B_{ij}e_{ij}^xA_{ij}e^{-B_{ij}r_{ij}}}{Q_i}+\sum_{j\neq i}\frac{e_{ij}^xB_{ij}^2A_{ij}\vec{e}_{ij}\cdot\vec{\mu}_je^{-B_{ij}r_{ij}}}{Q_iQ_j}\,, \tag{7}$$

where $\vec{\epsilon}_{i,\mathrm{loc}}$ is the local electric field at ion i, i.e., due to monopoles, applied fields, *and* dipoles. Calculations for diatomic molecules, where the electric fields are substantial, indicate that the linearization used to obtain the equilibrium equations results in only a small error.[21] Equilibrium equations resulting from minimization with respect to other components of the dipole moment of ion i or with respect to the dipole moments of other ions are easily obtained by inspection from Eq. (7).

The equations above for the dipole moments can be written formally as

$$\vec{\mu}_i=\underline{\alpha}_{\mathrm{eff}}\left(\vec{\epsilon}_{i,\mathrm{loc}}^{\,\mathrm{Coulomb}}+\vec{\epsilon}_{i,\mathrm{loc}}^{\,\mathrm{repulsion}}\right). \tag{8}$$

That is, the dipole moment on site i is a linear function of the usual Coulombic local field plus a local distortion field due to monopoles, the second term on the right-hand side of Eq. (7), and to dipoles, the third term on the right-hand side of Eq. (7). The effective polarizability tensor depends both on the free-ion polarizability and on the surroundings of the ion, as can be seen by examining the coefficients of μ_i^x, μ_i^y, μ_i^z in Eq. (7). Furthermore, it can be seen that as two ions approach one another, the polarizability is quenched by the overlap, thus preventing the polarization "catastrophe" discussed above.

The system of linear equilibrium equations, typified by Eq. (7), can be solved by matrix techniques.[17] In this calculation, the dipole moments in a region of the crystal surrounding the defect, roughly spherical in shape and containing 20–30 ions, were found in this fashion, while the dipole moments in the remainder of the crystal were obtained by the approximate method of Mott and Littleton.[18] In this approximation, the local fields of Eq. (8) are replaced by the monopole field alone, and the effective polarizability (for isotropic crystals) is given by

$$\alpha_i^{\mathrm{ML}}=\frac{\Delta}{4\pi}\left[(1-\epsilon^{-1})\Big/\left(\sum_{\text{unit cell}}(\alpha_j^e+\alpha_j^d)\right)\right](\alpha_i^e+\alpha_i^d) \tag{9}$$

where ϵ is the static dielectric constant, Δ is the unit-cell volume, and α_i is the polarizability, in the crystal, of the jth ion. The ionic polarizability is the sum of the electronic and displacement polarizabilities,[26] α_j^e and α_j^d, respectively. The Mott-Littleton approximation becomes exact in the limit that the monopole field is constant over the dimensions of the unit cell, thus as the distance from the defect becomes large.

The constants required for calculating the energy of polarization are the shell parameters Q, the free-ion polarizabilities α^0, and the electronic and displacement polarizabilities α^e and α^d, for the Mott-Littleton effective polarizabilities for each ionic species. The constants used in this calculation are collected in Table IV and were obtained as follows. The electronic polarizability of Al^{3+} was taken to be zero; the free-ion polarizability of O^{2-} was that of Pauling[27]; the crystal electronic polarizability of O^{2-} used in the Mott-Littleton approximation was obtained from the unit cell polarizability of Al_2O_3 reported by Tessman, Kahn, and Shockley[20] (with the Al^{3+} polarizability set to zero); the displacement polarizabilities for each ion were calculated with an Einstein rigid-ion model using the

TABLE IV. Parameters used in the calculation of polarization and Van der Waals's energy. Symbols are defined in Secs. III C and III D.

Parameter	Value
Q	2.24
$\alpha^0_{O^{2-}}$ (Å^3)	3.88[a]
$\alpha^e_{O^{2-}}$ (Å^3)	1.34[b]
$\alpha^d_{O^{2-}}$ (Å^3)	1.08
$\alpha^d_{Al^{3+}}$ (Å^3)	2.64
C (eV Å^6)	50.0

[a]Reference 27. [b]Reference 20.

repulsive parameters of Table III; the shell parameter Q for O^{2-} was obtained by matching the high-frequency dielectric constant, calculated with the Lorentz local-field approximation[28] and with Eq. (7), to the experimental value quoted by Tessman, Kahn, and Shockley.[20] The Lorentz local field is not strictly valid for noncubic crystals, but the value Q thus obtained is consistent with values obtained for O^{2-} by the analysis of a wide variety of experimental data for alkaline-earth oxide molecules and crystals.[21] The relationship of this value to the static dielectric constant will be discussed in Sec. IV D, and the sensitivity of the defect formation energies to the precise value of Q is discussed in Sec. V A.

D. Van der Waals's energy

The contribution of the Van der Waals's dispersion forces between the polarizable O^{2-} ions to the energy was included as

$$E_{\mathrm{VdW}} = -\frac{1}{2} \sum_{\substack{i,j \\ \text{oxygen ions}}}{}' \frac{C}{r_{ij}^6} . \tag{10}$$

The interaction constant was evaluated from the polarizability by the approximate method of Slater and Kirkwood[29] and is included in Table IV. The contribution of Van der Waals's interactions to the potential energy of ions in various sites in the perfect crystal is shown in Table II.

IV. PROPERTIES OF THE PERFECT CRYSTAL

In order to test the validity of the model described in Sec. III, calculations were made of several properties of the perfect crystal: cohesive energy, unit-cell volume and geometry, and bulk modulus. These properties are measures of the zeroth, first, and second derivatives with respect to distortion of the cohesive energy. In addition, an approximate value of the static dielectric constant was calculated. (Experimental data exist for the elastic constants and long-wavelength optic-mode frequencies which provide further tests of the model; calculations of these properties are in progress but still incomplete.)

A. Cohesive energy

The electrostatic monopole-monopole contribution to the cohesive energy, the negative of the first term of Eq. (6), has already been discussed in Sec. III A and is 189.1 eV. The repulsive, polarization, and Van der Waals's contributions were calculated as discussed in Sec. III B–III D and are −39.0, 0.1, and 2.0 eV, respectively. The total of these contributions yields a calculated cohesive energy of 152.0 eV compared with the experimental value[30] of 156.7 eV, a discrepancy of 3%.

B. Lattice parameter and crystal geometry

The stability of the model with respect to homogeneous deformations of the crystal was examined. The volume of the primitive unit cell of Fig. 2 was varied, scaling the lengths involved in the two-molecule basis to retain constant "shape," and the minimum energy was found at $a_0 = 5.25$ Å, compared with the experimental value[6] of 5.124 Å, a discrepancy of about 2%. The unit cell shape was varied by altering the unit cell angle and the various lengths in the basis, and discrepancies of a similar magnitude were found.

The basis of Fig. 2 can be slightly altered to make the Al_2O_3 structure become a hexagonal-close-packed array of oxygen ions with aluminum ions in the interstices,[6] i.e., the "ideal" structure shown in Fig. 1. Our calculations show that the distorted structure has a lower energy than the "ideal" structure, and thus that the distortions are not a consequence of covalent bonding, which is not accounted for in these calculations.

When a finite number of ions, placed in perfect crystal positions, were allowed to relax their positions and dipole moments in an identical fashion to the defect calculation it was found that slight shifts in position (about 0.1 Å compared with the ~ 2-Å interionic separation) resulted with a concomitant decrease in energy of 0.065 eV per relaxing ion (for between 26 and 36 relaxing ions). Such "perfect-crystal relaxations" do not occur for cubic crystals if the interatomic forces are not quite correct, being prevented by symmetry. In the defect calculations themselves, the ions were originally placed on perfect crystal positions, but the final relaxed positions and energies were corrected for the spurious "perfect-crystal relaxations."

C. Bulk modulus

The bulk modulus was obtained by calculating the cohesive energy as a function of volume and fitting a parabola to the results for small deviations from the minimum. The resulting modulus, 3.3×10^{12} dyn cm^{-2}, compares well with the experimental value[31] of 3.1×10^{12} dyn cm^{-2}.

D. Static polarizability

An approximate value of the response of Al_2O_3 to static electric fields was obtained by first deriving equilibrium equations, analagous to Eq. (7), by minimizing the energy with respect to both ionic dipole moments and small displacements from perfect-crystal positions. These equations were then solved under the assumption that the local field is identical at all ions, as it is when the Lorentz local-field approximation is valid. With this assumption, it can be shown that the static polarizability (the dipole moment divided by the local field) per Al_2O_3 unit α_s is given by

$$\alpha_s = 3\alpha^0 (Q-2)^2/Q^2 + \alpha_d \; , \tag{11}$$

where α^0 and Q are defined as in Sec. III C. α_d is the static polarizability of a rigid-ion Al_2O_3 lattice, and is found to be 4.89 Å^3 when calculated with the repulsive interactions of Table III and averaged over direction with respect to the hexagonal axis.

In the limit that the frequency of the applied field is too high for the positions of the ion core to respond, the polarizability α_∞ can be obtained from Eq. (7) and is given by

$$\alpha_\infty = 3(12/\alpha_d Q^2 + 1/\alpha_0)^{-1} \; . \tag{12}$$

As mentioned in Sec. III C, $Q = 2.24$ yields α_∞ equal to the value obtained from the refractive index and the approximation of the Lorentz local field. This value of Q in Eq. (11) yields $\alpha_s = 5.02$ Å^3 compared with 8.50 Å obtained from the static dielectric constant[32] and the Lorentz local field. To match the experimental value requires a value of $Q = 4.50$. This value is considerably higher than values for O^{2-} obtained for other oxides, [21] and furthermore leads to a negative value of the Schottky formation energy, as discussed in Sec. V A. These facts, together with the fact that the assumption of the Lorentz local field plays a larger role in the analysis of the static polarizability than in that for α_∞, suggest that the correct value of Q is nearer 2.24 than 4.5. The sensitivity of the defect energies to the value of Q is discussed in Sec. V A.

V. POINT-DEFECT PROPERTIES

The energies and lattice displacements associated with point defects were obtained as follows. Ions were removed or inserted in interstitial positions in a rigid, unpolarized (except for the polarization present in the perfect crystal) lattice, and the energy was calculated, using infinite crystal methods for the Madelung energy, as discussed in Sec. III A. A selected group of ions surrounding the defect, about 30 in number, were allowed to relax from their perfect crystal positions in small steps. During the relaxation process, the changes in the Madelung energy were computed using a finite crystallite, including the relaxing region, which contained 1855 ions, as discussed in Sec. III A. After each relaxation step, the dipole moments on the relaxing ions were obtained "exactly" by solving the set of Eq. (7) using a matrix technique. The total energy of the crystallite was then obtained from Eqs. (1), (3), (6), and (10), and the relaxation process was iterated until the energy was a minimum. The contribution due to the polarization of the remainder of the crystal which was not explicitly relaxed was calculated using the Mott-Littleton effective polarizabilities, Eq. (9), and the electric field due to the defect itself. The entire procedure was repeated with no defect present, and the resulting "perfect-crystal relaxation energy and displacements," discussed in Sec. IV B, were subtracted from the results computed with the defect present.

A. Defect-formation energies

The energy required to remove an ion from a lattice site or to insert one in an octahedral interstitial position in a rigid unpolarized crystal is obtained by inspection from Table II. The zero of potential energy in this table is for an ion removed to infinity, and the appropriate physical process for defect formation is removal to or from the crystal surface. Thus the entries in Table II must be corrected by the contribution of the ion in question to the cohesive energy, e.g., the energy to remove an Al^{3+} ion from the interior to the surface is 90.4−90.4/2 eV, while the energy required to remove an Al^{3+} ion from the surface to an interior octahedral position is 7.0+90.4/2 eV. The energies of formation of various vacancies and interstitials in the rigid, unpolarized lattice obtained in this fashion are collected in Table V along with the several contributions to the energy of relaxation and polarization and the consequent energy of formation in the relaxed polarized lattice for the shell parameter

TABLE V. Contributions to the formation energy of vacancies and interstitials in α-Al_2O_3 ($Q = 2.24$). (All energies in eV.)

Defect	Formation energy in rigid, unpolarized lattice	Relaxation energy Madelung	Repulsive	Van der Waals	Polar.	ΔE^a	Formation energy
Al^{3+} vacancy	45.2	−5.9	−3.1	−0.7	−28.5	+2.1	9.1
Al^{3+} interstitial	52.2	−39.2	+15.1	−1.0	−17.9	+1.7	10.8
O^{2-} vacancy	20.6	−15.9	+5.7	−0.9	−8.3	+2.3	3.5
O^{2-} interstitial	32.3	−14.6	+1.5	+0.6	−11.0	+1.7	10.5
Schottky-quintuplet formation energy, per defect							5.7
Aluminum-Frenkel-pair formation energy, per defect							10.0
Oxygen-Frenkel-pair formation energy, per defect							7.0

[a]Perfect-crystal relaxation energy. See Section IV B.

$Q = 2.24$.

It may be seen that the O^{2-} vacancy is energetically the most economical of the defects considered here, while the Al^{3+} interstitial requires the most energy. The formation energy, per defect, of the various electrically neutral defect families is: Schottky quintet, 5.7 eV; aluminum Frenkel pair, 10.0 eV; oxygen Frenkel pair, 7.0 eV. Thus it seems on the basis of this calculation that Schottky defects are the intrinsic thermodynamic point defects in α-Al_2O_3.

The sensitivity of the results to the number of ions explicitly allowed to relax and polarize was studied, and it was found that the Al^{3+} vacancy was the most sensitive to this quantity of the defects considered here, but the results obtained for 32 and 56 relaxing ions were essentially the same. Therefore it is believed that a sufficiently large number of ions was explicitly relaxed.

The sensitivity of the results to variations in the shell parameter Q was examined and the results are listed in Table VI. It may be seen that the Al^{3+} vacancy is rather sensitive, but that the other defects are insensitive to the exact value of Q, at least over a range of ± 0.1 around $Q = 2.24$. The Q dependence is essentially linear over this range, and the effect on the Schottky and Frenkel formation energies, per defect, may be summarized as

$$\begin{aligned} &\text{Schottky energy} = 5.7 - 5.0(Q - 2.24), \\ &\text{Al Frenkel energy} = 10.0 - 6.6(Q - 2.24), \quad (13) \\ &\text{Ox. Frenkel energy} = 7.0 - 1.3(Q - 2.24) \end{aligned}$$

(all energies are in eV). Assuming that these relationships are valid over a wider range of Q, it is seen that the Schottky formation energy becomes negative if Q exceeds 3.4, but between 2.24 and 3.4 the relative ordering of the energies of formation of the various defect families does not change. Thus it appears that the conclusion that the Schottky quintet is the energetically favored defect family does not depend on the exact value of Q.

The relaxation of the neighbors to the defects is somewhat more complex than is encountered in the alkali halides, owing to the lower symmetry of

TABLE VI. Shell-parameter dependence of the formation energy of vacancies and interstitials. (All energies in eV.)

Defect $Q =$	Formation energy 2.14	2.24	2.34
Al^{3+} vacancy	10.3	9.1	8.0
Al^{3+} interstitial	10.93	10.90	10.50
O^{2-} vacancy	3.6	3.5	3.45
O^{2-} interstitial	10.48	10.5	10.2

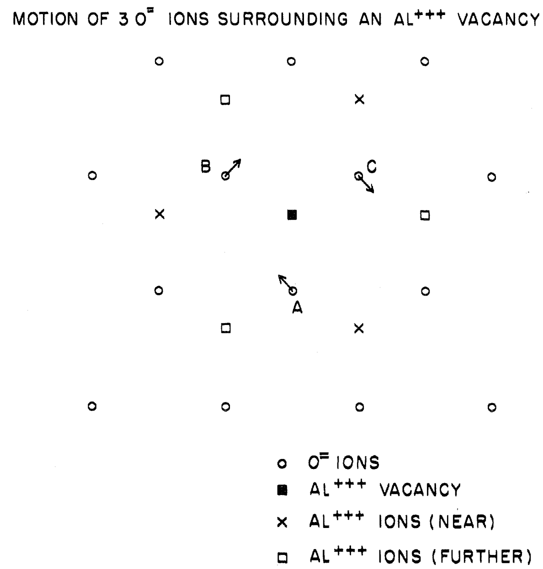

FIG. 7. Pinwheel distortion of O^{2-} neighbors to an Al^{3+} vacancy.

Al_2O_3. For example, the displacements of the oxygen neighbors to an Al^{3+} vacancy form a "pinwheel" pattern, as sketched in Fig. 7. However, as in the alkali halides, the basic pattern of relaxations is essentially outward from the defects, i.e., positive formation volumes, owing to the dominance of Coulombic interactions in the relaxations of vacancies. (A table of relaxation displacements for the various defects will be furnished by the authors upon request.)

B. Activation energies of defect motion

A systematic study of various paths for defect migration and of the relative mobilities of various defects has been initiated, and several preliminary results will be reported here. In each of the calculations described below, about 20 ions around the defect were allowed to relax explicitly, and the shell parameter Q was taken to be 2.24. In most cases the exact position of the jumping ion at the saddle point is not obvious, owing to the low symmetry, and a plausible guess was made. The following cases were investigated.

a. Migration of an Al^{3+} vacancy along the hexagonal axis. There are two neighbors to an Al^{3+} vacancy which lie along the c axis, one at 1.86 Å and one at 1.97 Å. In Fig. 1, for a vacancy at A, these neighbors are labeled 1 and 2, respectively. For a jump to neighbor 1, the obvious location of the jumping ion is in the center of the triangle of O^{2-} ions, and the migration energy for this jump is found to be 3.8 eV. For a jump of the vacancy to site 2, the location of the jumping ion at the saddle point will be at position I, and the activation energy is found to be 6.6 eV.

b. Migration of an Al^{3+} vacancy perpendicular to the hexagonal axis. The jump of an ion on site 3 to site A in Fig. 1 gives the vacancy a displacement with a component perpendicular to the c axis. Together with the short jump discussed above, this jump provides for three-dimensional diffusion of vacancies. Two possible saddle-point locations of the jumping ion were investigated. The first places the jumping ion halfway along a straight line joining the two sites. In this position, the two O^{2-} ions B and B_2 are nearest neighbors to the jumping ion, and the activation energy is found to be 3.8 eV. An alternate location for the jumping ion was investigated, at the center of the triangle of O^{2-} ions labeled B, B_1, and B_2. The activation energy in this location is, however, 6.5 eV and therefore this migration path from A to 3 is unfavorable compared with the direct jump originally chosen.

c. An O^{2-} vacancy jump to a nearest-neighbor position. The jump of an O^{2-} vacancy from site B to site B_1 in Fig. 1 was investigated. A vacancy taking jumps of this type remains in the basal plane, and at least one other type of jump is necessary to provide three-dimensional diffusion of the vacancy. If the jumping ion takes a straight-line path between these two sites, the energy maximum occurs at the halfway point, yielding an activation energy of 5.2 eV. If the jumping ion is not constrained to lie in the basal plane (determined by ions B_1, B_1', and B) and is permitted to relax in a direction perpendicular to this plane, the saddle point is found to be above this plane (nearer the Al^{3+} ion labeled 3), and the activation energy is 2.9 eV.

d. Al^{3+} interstitial migration. The migration of an Al^{3+} interstitial ion from site I to site I' in Fig. 1 was investigated by assuming the jumping ion to be in the symmetrical position S at the center of the triangle of O^{2-} ions when it is at the saddle point. With this assumption, the activation energy is 4.8 eV.

VI. SUMMARY OF RESULTS AND DISCUSSION

A polarizable point-ion shell model has been developed for α-Al_2O_3, in which it is assumed that the material is perfectly ionic. The repulsive interactions were determined by the modified Wedepohl method from free-ion wave functions. The only empirical parameter of the model is the shell parameter for the O^{2-} ion which was determined from the refractive index, and a value was found which is consistent with results for oxygen in alkaline-earth oxides. The model yields excellent results for the cohesive energy, unit cell volume and geometry, and bulk modulus. An approximate calculation utilizing the Lorentz local field yields a static dielectric constant that is appreciably too small, and it is not possible to choose a value of Q to match this quantity without making the crystal unstable with respect to vacancy formation. It is possible that the assumption of the Lorentz local field is the origin of this discrepancy.

The calculations of the formation of Al^{3+} and O^{2-} vacancies and interstitials at the octahedral site indicate that Schottky defects are energetically favorable relative to both aluminum and oxygen Frenkel pairs. This conclusion is independent of the exact value chosen for the shell parameter Q. The value of the Schottky formation energy obtained with $Q=2.24$, 5.7 eV per defect, is in fair agreement with the value of 4.1 eV implied by diffusion experiments.[1] Exact agreement is obtained with $Q=2.55$ [see Eq. (13)], a quite reasonable value. It must be recalled, however, that the interpretation of the experiments is not unambiguous.

The defect with by far the lowest formation energy is the O^{2-} vacancy. This implies[33] that near crystal surfaces where the electroneutrality condition is relaxed, a space charge layer will occur in which there are substantially more O^{2-} vacancies than are present in the interior where the higher energy of formation of Al^{3+} vacancies raises the energy per defect of the Schottky quintuplet by a factor of 2.

Preliminary results for activation energies of motion for the various defects suggest that O^{2-} vacancies are more mobile than Al^{3+} vacancies or interstitials. The calculated migration energy for O^{2-} vacancies in the basal plane, 2.9 eV, is in surprisingly good agreement with the experimental value of 2.5 eV from oxygen diffusion measurements[1] (for which the same qualifying remarks as before apply). Furthermore, the migration energy of the nonbasal jump of the O^{2-} vacancy has not yet been calculated. The migration energy of Al^{3+} vacancies was found to be 3.8 eV, which that for the direct migration of the interstitial was estimated to be about 5 eV, although the interstitialcy mechanism may provide a lower migration energy. No calculation was made for the migration energy of the O^{2-} interstitial. These preliminary calculations suggest that the experiments on the annealing of radiation damage[4] reflect the motion of O^{2-} vacancies.

---

†Research supported by the U. S. Atomic Energy Commission.

*Present address: Dept. of Applied Science, Brookhaven National Laboratory, Upton, N.Y. 11973.

[1]Y. Oishi and W. D. Kingery, J. Chem. Phys. 33, 480 (1960).

[2]A. E. Paladino and W. D. Kingery, J. Chem. Phys. 37, 957 (1962).

[3]G. M. Fryer, Trans. Brit. Ceramic Soc. 68, 185 (1969); 71, 231 (1972).

[4]R. S. Wilks, J. Nucl. Mater. 26, 137 (1968).

[5]B. S. Hickman and D. G. Walker, J. Nucl. Mater. 18, 197 (1966).

[6]R. W. G. Wycoff, *Crystal Structures*, 2nd ed. (Interscience, New York, 1967), Vol. 2, p. 6.

[7]R. H. Bartram (private communication).

[8]J. O. Artman and J. C. Murphy, Phys. Rev. 135, A1622 (1964).

[9]M. P. Tosi, *Solid State Physics*, edited by F. Seitz and D. Turnbull (Academic, New York, 1964), Vol. 16, p. 1.

[10]W. D. Wilson and C. L. Bisson, Phys. Rev. B 3, 3984 (1971).

[11]M. T. Robinson, in *Interatomic Potentials and Simulation of Lattice Defects*, edited by P. C. Gehlen *et al.* (Plenum, New York, 1972), p. 386.

[12]P. T. Wedepohl, Proc. Phys. Soc. Lond. 92, 79 (1967).

[13]R. G. Gordon and Y. S. Kim, J. Chem. Phys. 56, 3122 (1972); 61, 1 (1974).

[14]E. Clementi, IBM J. Res. Dev. 9, Suppl. 2 (1965).

[15]R. E. Watson, Phys. Rev. 111, 1108 (1958).

[16]M. L. Huggins and Y. Sakamoto, J. Phys. Soc. Jpn. 12, 241 (1957).

[17]T. A. Dellin *et al.*, Phys. Rev. B 1, 1745 (1970).

[18]N. F. Mott and R. W. Gurney, *Electronic Processes in Ionic Crystals*, 2nd ed. (Oxford U. P., Oxford, 1940).

[19]A. B. Lidiard and M. J. Norgett, in *Computational Solid State Physics*, edited by F. Herman, N. W. Dalton, and T. R. Koehler (Plenum, New York, 1972), p. 385.

[20]J. R. Tessman, A. H. Kahn, and W. Shockley, Phys. Rev. 92, 890 (1956).

[21]D. O. Welch and G. J. Dienes, in *Defects and Transport in Oxides: Proceedings of the Battelle Colloque* (to be published) and unpublished.

[22]M. J. L. Sangster, Solid State Commun. 15, 471 (1974).

[23]M. P. Tosi and M. Doyama, Phys. Rev. 160, 716 (1967).

[24]B. G. Dick and A. W. Overhauser, Phys. Rev. 112, 90 (1958).

[25]J. R. Hardy, Philos. Mag. 6, 27 (1961).

[26]J. W. Flocken and J. R. Hardy, Crit Revs. Solid State Sci. (CRC) 1, 605 (1970).

[27]L. Pauling, Proc. R. Soc. Lond. A 114, 191 (1927).

[28]C. Kittel, *Introduction to Solid State Physics*, 4th ed., (Wiley, New York, 1971), Chap. 13.

[29]J. C. Slater, *Quantum Theory of Molecules and Solids* (McGraw-Hill, New York, 1967), Vol. 3, Appendix 5.

[30]F. Seitz, *Modern Theory of Solids* (McGraw-Hill, New York, 1940), p. 83.

[31]J. B. Wachtman *et al.*, J. Res. Natl. Bur. Stds. A 64, 213 (1960).

[32]*Alumina as a Ceramic Material*, edited by W. H. Gitzen (Am. Ceram. Soc., Columbus, Ohio, 1970), p. 78.

[33]K. Lehovec, J. Chem. Phys. 21, 1123 (1953).